Quantitative analysis of enhanced light irradiance in waveguide-based fluorescent microarrays

Gabriel Sagarzazu, Mélanie Bedu, L. Martinelli, Nicolas Pelletier, Viatcheslav I. Safarov, C. Weisbuch, Thierry Gacoin, Henri Benisty

Quantitative analysis of enhanced light irradiance in waveguide-based fluorescent microarrays

Gabriel Sagarzazu[a,*], Mélanie Bedu[a], Lucio Martinelli[a], Nicolas Pelletier[a], Viatcheslav I. Safarov[a], Claude Weisbuch[b], Thierry Gacoin[b], Henri Benisty[c]

[a] *Genewave, XTEC, Ecole Polytechnique Campus, 91120 Palaiseau, France*
[b] *Laboratoire de Physique de la Matière Condensée, Ecole Polytechnique, CNRS, 91128 Palaiseau Cedex, France*
[c] *Laboratoire Charles Fabry, Institut d'Optique Graduate School, CNRS, Campus Polytechnique, 91127 Palaiseau Cedex, France*

Probing microarray assays in the presence of a hybridization mix retrieves precious information on hybridization kinetics. However, in common detection schemes, useful surface signals compete with the high supernatant background from labelled targets in the mix. A known solution consists in exciting specifically the microarray surface with evanescent fields. Configurations using planar optical waveguides to produce such fields are shown here to present also a dramatic excitation irradiance enhancement at the guide/surrounding matter interface. We compare theoretically and experimentally a guided excitation with a classical external excitation. A full electromagnetic analysis predicts an irradiance increase higher than 10^4 for adequately tailored waveguides. We deposited high-index TiO_2 sol–gel waveguides on glass substrates according to best simulations. Quantitative enhancement analysis exploiting actual biological fluorescent spots perfectly confirms the irradiance amplification effect of a thin waveguide. The impact of amplification on the design of biochip readers is discussed since it leaves ample margin for simple and low-cost light couplers, advantageous in affordable readers and sensor systems.

1. Introduction

Combinatorial assays are potent tools for biological analysis, providing avenues to explore gene and protein functions in living organisms (Van Hal et al., 2000; Lueking et al., 1999). Several detection techniques are currently exploited. Label-free detection methods (e.g. Surface Plasmon Resonance (SPR), ellipsometry, ...) enable spot detection in the presence of a mix during hybridization, and thus the ability to follow hybridization kinetics or to optimize assay parameters (temperature, composition, ...). Labelled molecules are suspected to influence the binding process altering the information (Schmitt et al., 2007).

However, these methods, generally mass-sensitive, offer a poor contrast if the target size or amount becomes low. In contrast, for fluorescent or radioactive detection, the hybridization event signals only arise from labels linked to the biomolecules, without background. Among these selective techniques, fluorescence is the most used because of its simplicity (Schäferling and Nagl, 2006; Schena, 2003) and innocuity.

The sensitivity of standard top-reading fluorescence schemes is quite degraded by the hybridization mix: the reading step is thus usually performed after hybridization, washing and drying. But for fine monitoring of biological assays or shorter time to results, it is very desirable to detect spots signals in the presence of a hybridization mix. With an external excitation source, the whole mix above the spots strongly fluoresces, generating a large background and jeopardizing spot detection. These systems can regain their superior sensitivity if the microarray is excited by evanescent waves (Rowe Taitt et al., 2005) which explore only 100 nm above the surface. The spots are then well excited, unlike most of the labelled species floating above the evanescent field. Hybridized species at the surface appear with high contrast. Preferred techniques are Total Internal Reflection Fluorescence (TIRF), and optical waveguides (Lehr et al., 2003; Duveneck et al., 1997). Their advantages in terms of sensitivity are well documented (Klotz et al., 1998; Rowe et al., 1999; Kunz and Cottier, 2006).

In the present letter we quantify another aspect of thin waveguide-based excitation: a strong enhancement of the electromagnetic field at the guide/surrounding matter interface. Calculations and measurements on biological objects show that this enhancement can reach several orders of magnitude ($\geq 10^4$). We eventually discuss the impact of this enhancement on the design of

* Corresponding author.
E-mail address: gabriel.sagarzazu@genewave.com (G. Sagarzazu).

compact and cheap high-sensitivity readers (light source, coupling in the chip, fluidics).

2. Materials and methods

2.1. Planar optical waveguides

Waveguide physics is key to our study. The predicted enhancement of irradiance at the guide interface is experimentally assessed, and confirmed by measurements on a TiO_2 sol–gel guiding layer deposited on a glass substrate (refractive index $n_{sub}(\lambda) = 1.52$) using spin-coating techniques (fabrication details will be given elsewhere). This easy in-house elaboration technique gives access to various high refractive indices and guide thicknesses. It also lends itself to low-cost fabrication.

The layer thickness and refractive index are measured by spectroscopic ellipsometry. The process is optimized in order to obtain a guiding layer thickness between 100 and 130 nm and refractive indices between 1.8 and 2. Such indices are rather low for this oxide but the fabrication process was also optimized to get a material microstructure limiting propagation losses.

2.2. Microarray preparation

In order to demonstrate the guided excitation advantage in a biological assay, we fabricated a microarray on our TiO_2 waveguides. Our aim is to assess the irradiance at the superstrate/guide interface by comparing the fluorescence of biological spots between an external and a guided excitation. From a photonic viewpoint, it is safer to use control spots instead of reading the microarray after hybridization. This method preserves the reproducibility, and ensures large signals and high experimental contrast. We thus directly deposited Alexa 647^{TM} labelled actin oligomers on the waveguide surface (few-nanometers-thick spots, see details in Supplementary material).

We underline that we did not realize a hybridization step but the fluorescent spots we deposited are good models of those that are generally detected in conventional assays.

2.3. Experimental setup

As shown in Fig. 1(a), we couple light from a collimated He–Ne laser (excitation wavelength $\lambda = 633$ nm) into the waveguide through a conventional 90° prism coupler whose index is $n_{prism} = 1.91$ (Tien and Ulrich, 1970; Ulrich, 1970). At the residual air gap, a fraction η_C of the power is coupled into the waveguide, and is optimized by scanning the incidence angle θ.

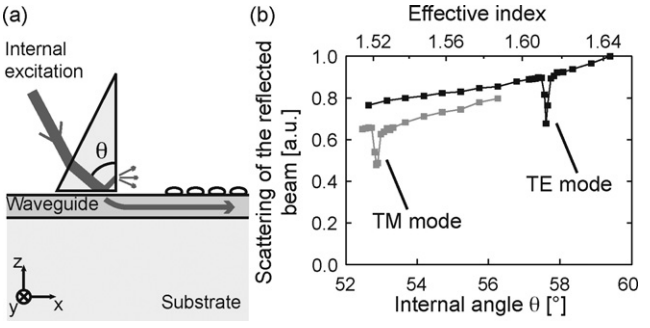

Fig. 1. (a) Coupling setup used for the internal excitation of labelled oligomers at the microarray surface. Light not coupled into the guide scatters at the unpolished prism face. (b) Typical measurement of scattered uncoupled light as a function of internal angle θ. Dips correspond to guided modes (effective indices $n_{\text{eff}}^{\text{TE}} = 1.61$ and $n_{\text{eff}}^{\text{TM}} = 1.52$).

Because measuring directly the coupling efficiency η_C commonly entails inaccuracies (Caballero-Calero et al., 2007) we rather record here the intensity variation of the prism/guide interface reflection, proportional to $(1-\eta_C)$. We do this by collecting the scattered light generated when this reflected beam impinges on the vertical unpolished prism face. The area and collection of this scattered light are such that speckle is no trouble.

Other measurements are more conventional. The guiding losses caused by waveguide defects (index fluctuations, interface roughness) are quantified with the "scattering detection method" (Nishihara et al., 1989), imaging the spatial decay of scattered light onto a charge-coupled-device (CCD). Finally, we couple this imaging system with a bandpass emission filter, yielding fluorescence images in the label emission band.

3. Results

3.1. Electromagnetic analysis

We first introduce a figure-of-merit (*FOM*) that quantitatively accounts for the gain in excitation efficiency. For a given total excitation power, if an area of 1 cm^2 is excited (i) with an external beam or (ii) with a guided wave, the *FOM* is merely the ratio of the corresponding irradiances I at the spots level (I being the square of electric field $|E|^2$):

$$FOM = \frac{I_{\text{SPOT,GUIDED}}}{I_{\text{SPOT,EXTERNAL}}} \tag{1}$$

Our study is restricted to applications where fluorophores lie well within the evanescence depth (~100 nm). This encompasses a large majority of techniques that use a similar localized excitation like TIRF or SPR. Within this assumption, at first order, the *FOM* reads:

$$FOM = \frac{I_{\text{AIR/GUIDE INTERFACE,GUIDED}}}{I_{\text{AIR/GUIDE INTERFACE,EXTERNAL}}} \tag{2}$$

For a typical ~100 nm evanescence depth into the aqueous solution, the irradiance for a fluorophore floating at only 1 μm height plummets by a factor 10^{-9} from the surface value.

Elementary geometric considerations dictate a rough *FOM* estimate. For free-space external excitation, the total exciting power is spread over 1 cm^2, against only ~1 cm × 1 μm for guided schemes (1 μm is an upper limit of a guided wave effective width), thus providing the essential source of the gain in irradiance of several orders of magnitude (~10^4). The 1 cm^2 choice is a typical biosensor area for real-time hybridization study of large spot collections (Van Hal et al., 2000; Lehr et al., 2003).

We now perform an exact calculation based on standard optical guided wave theory (Yeh, 1988). The waveguide consists of a glass substrate ($n_{sub}(\lambda) = 1.52$) coated by a high-index layer (optical index $n_g(\lambda)$, thickness t). The superstrate is provisionally air ($n_{sup} = 1$) and we present results for a core index $n_g(\lambda) = 1.95$. Fig. 2 shows the irradiance (in mW/cm^2) at the air/guide interface versus the waveguide thickness t for a total power of 1 mW carried by each of the waveguide modes. For free-space excitation, the reference surface irradiance reads 1 mW/cm^2, hence Fig. 2 directly plots the waveguide FOM.

We first note the appearance of a well-defined maximum for each mode, at a thickness just above the mode cut-off. The largest maximum, $FOM = 2.2 \times 10^4$, arises for thicknesses t comprised between 105 nm and 115 nm, which corresponds to a monomode guide for a given polarization (the cut-off is around $t = 60$ nm). The higher modes for thicker layers beat the fundamental mode at a given width, but their peak values are weaker than the fundamental mode maximum. The overall decrease

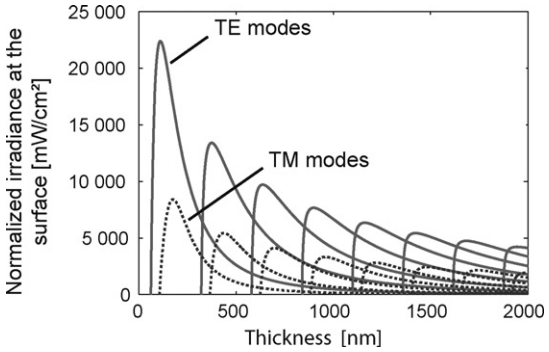

Fig. 2. Irradiance at the air/core interface for a guided internal excitation as a function of high-index layer thickness t. Each mode carries a power density of 1 mW/cm (1 mW per 1 cm width).

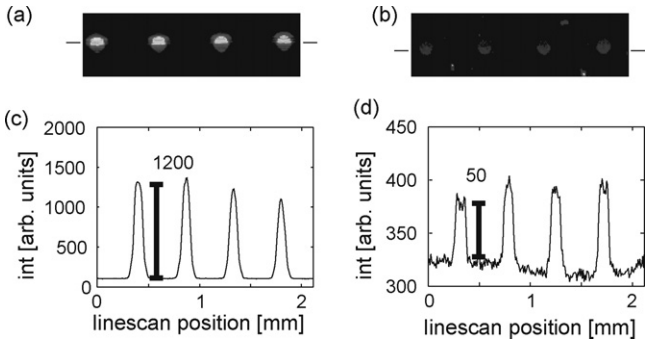

Fig. 3. Fluorescence images of biological spots for (a) a guided internal excitation and (b) an external excitation. (c) and (d) linescans of these spots [respectively (a) and (b)] show an irradiance gain in favour of guided wave excitation. Correcting these data for experimental parameters (See supplementary material), the fluorophore irradiance is 1.2×10^4 times larger for waveguide excitation.

at large thickness is expected since a TIRF-like situation with thickness in the millimeter/centimeter range would feature a *FOM* value approaching unity. The asymmetry (superstrate index $n_{sup} = 1$ and substrate index $n_{sub} = 1.52$) induces an important mode profile asymmetry sizably spoiling the *FOM*. Simulations logically confirm a reduced penalty for increased core refractive index, symmetry being restored in relative terms. We thus observe that the higher the guiding layer index, the larger the *FOM*. Fortunately, in aqueous solutions, the asymmetry is also reduced, yielding a notable *FOM* increase, over 30% for a $n_{sup} = 1.33$ superstrate. Thus, the best *FOM* could reach about 3×10^4.

4. Experimental

From the above electromagnetic trends, the TiO_2 sol–gel synthesis is optimized toward a layer refractive index $n_g(\lambda = 633\,\text{nm}) = 1.95$ and a 108 nm thickness. Since the *FOM* depends only on optogeometrical waveguide parameters, the experimental obtainment of a high *FOM* may rely on other solutions (e.g. Ta_2O_5, a recognized high-index optical coating material).

To assess the *FOM* value, we compare the spots fluorescence intensity at the microarray surface between external and guided excitation. We underline that the *FOM* was introduced as an intrinsic parameter of the waveguide architecture, deliberately not taking into account the various setup-dependent losses. In other words, if L represents the product of all setup losses, and $L = 0$ for the basic external excitation geometry, the irradiance ratio between external and guided excitation schemes reads:

$$\frac{I_{\text{AIR/GUIDE INTERFACE,GUIDED}}}{I_{\text{AIR/GUIDE INTERFACE,EXTERNAL}}} = FOM \cdot (1 - L) \tag{3}$$

In our case, losses are essentially induced by imperfect light coupling and by genuine guiding losses (scattering of coupled excitation along the guided path).

We first measure the coupling efficiency selected TE polarization throughout to achieve the largest *FOM*. As said, we measure the intensity of uncoupled, reflected light, further scattered by the unpolished prism face, as a function of the internal angle θ. The observed neat dips, Fig. 1(b), reveal phase-matching coupling conditions. Coupling requires good angular accuracy, the typical dip width being around $\Delta\theta \approx 0.2^\circ$. We typically get $\eta_C \approx 20$–25%. Measurements fluctuate slightly among guide-prism setup: we evaluate η_C for each of them.

Then, the measured guiding losses range between 1.0 ± 0.5 dB/cm and 3.0 ± 0.5 dB/cm for different samples, the lower bound being limited by our detection sensitivity.

Fig. 3 shows the raw data of the microarray excitation comparison. The experimental *FOM* is deduced from the following equation:

$$FOM = \frac{F_{\text{guided}} \cdot P_{\text{external}} \cdot D_{\text{guided}} \cdot \tau_{\text{external}}}{F_{\text{external}} \cdot (P_{\text{guided}}/10^{OD}) \cdot D_{\text{external}} \cdot \tau_{\text{external}} \cdot \eta_c \cdot 10^{-\alpha \cdot d/10}} \tag{4}$$

where $F_{\text{guided/external}}$ is the spots fluorescence signal (for guided/external excitation), $P_{\text{guided/external}}$ is the total excitation power, i.e. the laser output, $D_{\text{guided/external}}$ is the beam size, $\tau_{\text{guided/external}}$ is the CCD exposure time, η_C the coupling efficiency, α the attenuation coefficient (dB/cm) that represents guiding losses, d the distance between the coupling point and the spots and OD is the neutral filter density inserted for guided excitation (we attenuate laser power to avoid CCD saturation and fluorophore bleaching).

The coupling efficiency of 21% is retrieved from a posterior angular scan, to avoid bleaching. We analyze spots located at 1 cm away from the coupling area, taking 3 dB guiding losses into account. The guided beam width of 1.5 mm ensures homogeneous spot excitation while the external excitation is equivalent to a power P_{external} spreading over a 1 cm × 1 cm area.

This analysis provides a figure of merit $FOM = 1.2 \times 10^4$ which is quite close to the predicted value of $FOM = 2.2 \times 10^4$. This result confirms experimentally the large enhancement of the electromagnetic field at the waveguide interfaces. In the present experimental demonstration, the superstrate is air ($n = 1$). As said earlier, with a superstrate of index ~1.33 (aqueous hybridization mix) a further 30% *FOM* increase is expected.

5. Discussion

If the recovery of the sensitivity in the presence of a fluorescent mix is a major asset of waveguide-based systems, it must be emphasized that the irradiance enhancement by confinement effects also brings important instrumental advantages. This is especially true since a generic critical point of waveguide-based microarray techniques is related to the light coupler. We show in this paper that a large *FOM* enables a simplified coupling function for this class of apparatus.

Duveneck et al. described the mechanical requirements for systems that use gratings. The angle of incidence must be adjusted very precisely ($\Delta\theta$ is between 0.01° and 0.1°) to attain the phase-matching condition (Duveneck et al., 2002) and we confirmed close requirements for prism couplers (Fig. 1(b)). Such an alignment is needed before each measurement since a new biochip comes in the reader for each new sample.

Theoretically, it is always possible to compensate for coupling losses through increased excitation power or detector exposure. In practice, the high *FOM* value (>10^4) we assessed for adequately

tailored waveguides is a more elegant and efficient method that allows relaxing the requirements for the light coupling.

Even with imperfect couplers, one could still have an overall enhancement thanks to the large figure of merit. One of many possible low-cost solutions could notably be nano-imprinted gratings with relaxed tolerances. Another simple option is excitation of waveguide modes by optically pumped fluorescent species directly incorporated into a section of the waveguide. The fluorescence light, well captured in guided modes, subsequently excites the microarray spots at the surface. Even if this coupling scheme leads to sizable losses (e.g. fluorescence efficiency, reabsorption, radiation into air or into the substrate), this scheme still allows acceptable excitation of the spots thanks to the large *FOM* value of guided modes. Even in the presence of losses induced by the traversal of the seal of a fluidic cell, liable to scatter the guided wave, the large intrinsic *FOM* still leads to a large absolute excitation efficiency. Hence, in many schemes, the power at the surface remains at a high enough level for easy measurements if typical laser powers of 1–50 mW are used. High-brightness light-emitting diodes (LEDs) could also be the primary source when using embedded fluorescent internal sources.

6. Conclusion

A waveguide-based configuration appears to bring several advantages for fluorescence microarray reading in the presence of the fluorescent biological hybridization mix, or of other fluorescent liquids. It permits not only preserving a good contrast and sensitivity of spot detection, but also an efficient use of exciting light for thin waveguides.

Thus, even though such an irradiance enhancement seems to be regarded as secondary in the literature, the huge *FOM*, that we assessed both theoretically and experimentally for adequately tailored waveguides, strongly relaxes the requirements on the optical microarray hardware design. Schemes with cheap and simple optical sources and simple optical coupling elements can be devised, and a few avenues have been proposed. Engineering requirements on fluidics-related demands (e.g. traversal of waveguide light beneath seals, thickness of supernatant) can also be reconsidered thanks to this optimal use of excitation light.

Acknowledgements

The authors acknowledge the help of Genewave team. This work was partly supported by French ANR 2005 “BRIO+” project.

References

Caballero-Calero, O., Camicero, J., Alcazar, A., De la Paliza, G., García-Cabañes, A., Carrascosa, M., Cabrera, J.M., 2007. J. Appl. Phys. 102, 074509.

Duveneck, G.L., Pawlak, M., Neuschäfer, D., Bär, E., Budach, W., Pieles, U., Ehrat, M., 1997. Sens. Actuators B 38–39, 88–95.

Duveneck, G.L., Abel, A.P., Bopp, M.A., Kresbach, G.M., Ehrat, M., 2002. Anal. Chim. Acta 469, 49–61.

Klotz, A., Brecht, A., Barzen, C., Gauglitz, G., Harris, R.D., Quigley, G.R., Wilkinson, J.S., Abuknesha, R.A., 1998. Sens. Actuators B 51, 181–187.

Kunz, R.E., Cottier, K., 2006. Anal. Bioanal. Chem. 384, 180–190.

Lehr, H.P., Brandenburg, A., Sulz, G., 2003. Sens. Actuators B 92, 303–314.

Lueking, A., Horn, M., Eickhoff, H., Büssow, K., Lehrach, H., Walter, G., 1999. Anal. Biochem. 270, 103–111.

Nishihara, H., Haruna, M., Suhara, T., 1989. Optical Integrated Circuits. McGraw-Hill, New York.

Rowe, C.A., Tender, L.M., Feldstein, M.J., Golden, J.P., Scruggs, S.B., MacCraith, B.D., Cras, J.J., Ligler, F.S., 1999. Anal. Chem. 71, 3846–3852.

Rowe Taitt, C., Anderson, G.P., Ligler, F.S., 2005. Biosens. Bioelectron. 20, 2470–2487.

Schäferling, M., Nagl, S., 2006. Anal. Bioanal. Chem. 385, 500–517.

Schmitt, K., Schirmer, B., Hoffmann, C., Brandenburg, A., Meyrueis, P., 2007. Biosens. Bioelectron 22, 2591–2597.

Schena, M., 2003. Microarray Analysis. Wiley, New Jersey, Hoboken.

Tien, P.K., Ulrich, R., 1970. J. Opt. Soc. Am. 60, 1325–1337.

Ulrich, R., 1970. J. Opt. Soc. Am. 60, 1337–1350.

Van Hal, N.L.W., Vorst, O., Van Houwelingen, A.M.M.L., Kok, E.J., Peijnenburg, A., Aharoni, A., Van Tunen, A.J., Keijer, J., 2000. J. Biotechnol. 78, 271–280.

Yeh, P., 1988. Optical Waves in Layered Media. Wiley, New York.